

UNIVERSITY OF CALIFORNIA

Los Angeles

**Nature-Inspired Optimization Techniques Applied to
Antennas for Wireless Communications and Radar**

A thesis submitted in partial satisfaction
of the requirements for the degree
Master of Science in Electrical Engineering

by

Joshua Michael Kovitz

2012

© Copyright by
Joshua Michael Kovitz
2012

ABSTRACT OF THE THESIS

**Nature-Inspired Optimization Techniques Applied to
Antennas for Wireless Communications and Radar**

by

Joshua Michael Kovitz

Master of Science in Electrical Engineering

University of California, Los Angeles, 2012

Professor Yahya Rahmat-Samii, Chair

In this work, two nature-inspired optimization techniques, namely Particle Swarm Optimization (PSO) and Covariance Matrix Adaptation Evolution Strategy (CMAES), are presented. Some comparisons are made between the two algorithms in different applications and different optimization problems. First, a comparison of each algorithm in resource limited problems is demonstrated using mathematical functions. Next, a comparison is shown between the two algorithms for a real-world antenna design problem for radar systems. In particular, a weather radar antenna array element is optimized using two different approaches, and some suggestions are made for antenna designers hoping to implement dual polarized antenna arrays for new use in weather radar systems. In the last half of this work, the Particle Swarm algorithm is applied to two other antenna systems. The first application of PSO investigates the use of a smooth contour septum design in circular waveguide for possible use in high power microwave systems. Similar antenna performance compared to a stepped septum in circular waveguide is demonstrated using the Sigmoid function contour. PSO is also applied on two newly proposed reconfigurable E-shaped patch antenna designs. Two reconfigurability mechanisms are introduced, namely a polarization (RHCP/LHCP) reconfigurable design and a frequency reconfigurable design. Both designs are optimized using a simple MEMS circuit model for fast optimization, and possible bias network implementations are discussed. Wideband patch designs are realized with these optimizations, and prototypes are fabricated and measured to validate these designs.

The thesis of Joshua Michael Kovitz is approved.

Tatsuo Itoh

Lieven Vandenberghe

Yahya Rahmat-Samii, Committee Chair

University of California, Los Angeles

2012

*To my sweet wife Anel, who encouraged me in the difficult times
and rejoiced with me in my accomplishments*

TABLE OF CONTENTS

| | | |
|----------|--|-----------|
| 1 | Introduction | 1 |
| 1.1 | Motivation | 2 |
| 1.2 | Optimization in Electromagnetics | 8 |
| 1.3 | Performance Evaluation in Antenna Design | 14 |
| 1.4 | Outline of Work | 19 |
| 2 | Nature-Inspired Optimization Techniques | 22 |
| 2.1 | Particle Swarm Optimization (PSO) | 28 |
| 2.1.1 | Real-valued Particle Swarm Optimization | 31 |
| 2.2 | Covariance Matrix Adaptation Evolutionary Strategies (CMAES) | 36 |
| 2.3 | Applications in Constrained Optimization Problems | 47 |
| 2.4 | Convergence Analysis using Mathematical Functions | 51 |
| 2.5 | Implementation | 57 |
| 3 | Comparison Between PSO and CMAES | 59 |
| 3.1 | Mathematical Function Comparison | 59 |
| 3.2 | Nonuniform Antenna Array Optimization | 71 |
| 4 | Optimization of Polarimetric Radar Systems | 78 |
| 4.1 | Antennas for Polarimetric Radar Systems | 81 |
| 4.2 | Optimization of Cross Polarized Fields | 85 |
| 4.2.1 | Optimization Problem Development | 85 |
| 4.2.2 | PSO and CMAES Results and Comparison | 89 |
| 4.3 | Direct Optimization of Bias Weighting Factors | 94 |

| | | |
|----------|--|------------|
| 4.3.1 | Optimization Problem Development | 94 |
| 4.3.2 | PSO and CMAES Results and Comparison | 97 |
| 4.4 | Some Final Comparisons and Discussion | 102 |
| 5 | Smooth Contour Septums for High Power Microwave Systems | 108 |
| 5.1 | Septum Design and Current Issues | 110 |
| 5.2 | Sigmoid Function and Its Properties | 113 |
| 5.3 | Formulation of the Optimization Problem | 117 |
| 5.3.1 | Stepped Septum Optimization | 117 |
| 5.3.2 | Sigmoid Septum Optimization | 129 |
| 5.4 | Final Design Comparison | 135 |
| 6 | MEMS Reconfigurable E-Shaped Patch Antennas | 138 |
| 6.1 | Introduction to E-Shaped Patch Antennas | 139 |
| 6.2 | Development of a Simple MEMS Model | 143 |
| 6.3 | Circular Polarization Reconfigurable E-Shaped Patch | 153 |
| 6.3.1 | Concept Design | 153 |
| 6.3.2 | Applying Particle Swarm Optimization | 157 |
| 6.3.3 | Results and Measurements | 163 |
| 6.4 | Frequency Reconfigurable E-Shaped Patch | 168 |
| 6.4.1 | Physical Principles | 170 |
| 6.4.2 | Optimization for Wideband Designs | 173 |
| 6.4.3 | Final Designs | 177 |
| 6.5 | Bias Network Development | 181 |
| 6.6 | Further Discussion | 192 |

7 Conclusions 193

References 196

LIST OF FIGURES

| | | |
|-----|--|----|
| 1.1 | Depiction of the basic blocks of a wireless communication system | 3 |
| 1.2 | Basic bistatic radar system detecting a scattering object | 4 |
| 1.3 | Representation of design parameters with uniformly spaced testing points for 1 dimension, 2 dimensions, and 3 dimensions | 7 |
| 1.4 | Typical flowchart for an optimization algorithm for electromagnetic design problems | 10 |
| 1.5 | Interface configuration for the simulator and the optimization engine | 12 |
| 1.6 | Transmitting and receiving antennas in free space | 16 |
| 1.7 | Outline of work in this thesis. The introduction to optimization within electromagnetics is given in Chapter 1. The comparison of the algorithms is given in Chapters 3 and 4. The septum design and the reconfigurable E-shaped patch designs are given in Chapters 5 and 6, respectively. The final conclusions are given Chapter 7. | 20 |
| 2.1 | Illustration in the differences between Unimodal and Multimodal functions for optimization | 24 |
| 2.2 | A short list of different optimization algorithms and their classification | 27 |
| 2.3 | A graphical depiction of Kennedy and Eberhart's original simulation model which inspired Particle Swarm Optimization | 30 |
| 2.4 | Pseudocode implementation of the Real-valued Particle Swarm Optimization technique which minimizes the fitness function | 34 |
| 2.5 | Boundary conditions applied to a two-dimensional problem | 35 |
| 2.6 | Basic evolutionary concept behind Evolutionary Strategies | 37 |
| 2.7 | Ellipsoidal function $f(x, y) = (x/3)^2 + y^2$ being optimized with a simple best-child evolution strategy. This is a simplified algorithm to explain CMAES. | 40 |
| 2.8 | Plot of the weights for finding the new population centroid $\langle \vec{x} \rangle^{i+1}$ using equation 2.13 | 43 |

| | | |
|------|---|----|
| 2.9 | Pseudocode implementation of the Covariance Matrix Adaptation Evolution Strategy technique which minimizes the fitness function | 46 |
| 2.10 | Visualization of the Feasible and Infeasible regions | 49 |
| 2.11 | Application of PSO on a 2-dimensional Schwefel function | 54 |
| 2.12 | Comparison of Different Averaging Procedures | 56 |
| 3.1 | Two dimensional versions of the six testing functions | 62 |
| 3.2 | Optimization results when $N = 50$ versus <i>iterations</i> for the mathematical test functions | 64 |
| 3.3 | Optimization results when $N = 50$ versus <i>function evaluations</i> for the mathematical test functions | 65 |
| 3.4 | Optimization results when $N = 5$ versus <i>iterations</i> for the mathematical test functions | 68 |
| 3.5 | Optimization results when $N = 5$ versus <i>function evaluations</i> for the mathematical test functions | 69 |
| 3.6 | Geometry used for the symmetrical nonuniform antenna array to be optimized with PSO and CMAES. The outer elements are located at $x = \pm 2.75\lambda_0$ and the other element positions are to be optimized | 72 |
| 3.7 | Comparison of optimization results between PSO and CMAES for the nonuniform array with 12 elements | 76 |
| 3.8 | Final design geometry provided from CMAES. The resulting design from PSO is almost identical to the one depicted. A 12 element uniform array with $\lambda_0/2$ element spacing is also shown in gray as a reference. | 77 |
| 4.1 | Illustration of the basic polarimetric weather radar used to measure properties of the precipitation | 79 |

| | | |
|------|--|-----|
| 4.2 | Ludwig's 2nd definition of copolarized (red vectors) and cross polarized (blue vectors) radiation from an antenna having a main lobe in the X direction with Y-directed currents | 82 |
| 4.3 | Stacked patch antenna configuration for possible use in weather radar systems . | 83 |
| 4.4 | Exploded view of the stacked patch used in the optimization | 84 |
| 4.5 | Coordinate system used for measuring the crosspolar fields in the cross polarized field optimization (XPFO) | 86 |
| 4.6 | Convergence for the XPFO problem | 91 |
| 4.7 | S_{11} response for the final PSO design (similar characteristics are observed with the CMAES design) | 93 |
| 4.8 | Radiation patterns of the final optimized stacked patch antenna design in the principle planes | 93 |
| 4.9 | Coordinate system used for determining the crosspolar fields in the bias weighting factor optimization (BWFO) | 96 |
| 4.10 | Convergence for the BWFO problem | 99 |
| 4.11 | S_{11} response for the final PSO and CMAES designs | 100 |
| 4.12 | Radiation patterns of the final optimized stacked patch antenna designs in the principle planes | 100 |
| 4.13 | S_{11} response for the final PSO and CMAES designs | 104 |
| 4.14 | Comparison of the radiation patterns at 2.85 GHz for the final optimized stacked patch antenna designs of the two different optimization approaches | 104 |
| 5.1 | Reflector antenna system using circular polarization duplex | 109 |
| 5.2 | Septum polarizer within a circular waveguide cross section | 110 |
| 5.3 | Decomposition of the port 1 and port 2 excitation into the even and odd modes, which are responsible for generating the TE_{11} as well as the rotated TE'_{11} , respectively | 111 |

| | | |
|------|---|-----|
| 5.4 | Septum and circular horn design; the design to the left uses the sigmoid function and the one to the right uses a stepped septum | 113 |
| 5.5 | Sigmoid function and its Taylor expansion about the point $x = L$ | 114 |
| 5.6 | The effect of each parameter on the sigmoid function | 115 |
| 5.7 | The effect of each parameter on the curvature of the sigmoid function | 116 |
| 5.8 | Sigmoid summation to represent the septum contour | 118 |
| 5.9 | Top view of the stepped (dashed) and sigmoid (solid) septums | 119 |
| 5.10 | Stepped septum design for the 5-step case | 120 |
| 5.11 | Maximum space that could be possibly occupied by the septum design (using the max/min value for L_i) | 122 |
| 5.12 | Visualization of a circularly polarized wave | 123 |
| 5.13 | Convergence of the six-stepped septum | 126 |
| 5.14 | Scaled drawing of the final optimized six-step septum design | 126 |
| 5.15 | Performance of the optimized stepped septum design | 128 |
| 5.16 | Scaled drawing of an oversized sigmoid function within a waveguide for $H_1 = H$, $L_1 = L/2$, and $C_1 = 10$ | 129 |
| 5.17 | Scaled drawing of the worst case sigmoid allowable within the septum design area where $H_1 = H$, $L_1 = L/2$, and $C_1 = L/2H$ | 130 |
| 5.18 | Convergence of the six-sigmoid septum | 133 |
| 5.19 | Scaled drawing of the final optimized six-sigmoid septum design | 133 |
| 5.20 | Performance of the optimized sigmoid septum design | 134 |
| 5.21 | Comparison of the performance of the optimized stepped septum design and the optimized sigmoid septum design | 136 |
| 6.1 | Demonstration of the simplicity of a coaxial probe-fed rectangular patch | 140 |
| 6.2 | Circuit model of the patch input port | 141 |

| | | |
|------|---|-----|
| 6.3 | Top view of the U-slotted and the E-shaped patch antenna topologies | 142 |
| 6.4 | Depiction of the possible resonant modes that can occur in the E-shaped patch antenna | 143 |
| 6.5 | Simple illustration of a MEMS switch | 144 |
| 6.6 | Several possible implementations of the MEMS model within a full wave electromagnetics simulator | 146 |
| 6.7 | S_{11} comparison of the ideal case between simulation and measurement | 148 |
| 6.8 | Fabricated antennas and simulation topology to measure the ideal switch case . | 148 |
| 6.9 | S_{11} comparison of the ideal switch measurement versus the wirebonded MEMS implementation | 149 |
| 6.10 | Implementation of the MEMS switches into the E-shaped patch antenna optimized with the ideal switch model | 149 |
| 6.11 | Comparison of the S_{11} from the wirebonded MEMS measurement with the full MEMS model and the circuit model using $C = 80\text{pF}$ | 151 |
| 6.12 | Models for comparison to the measured wirebonded MEMS performance | 151 |
| 6.13 | Circuit model used in the optimization for the reconfigurable E-shaped patch antenna | 152 |
| 6.14 | Asymmetric slots in the E-shaped patch antenna creates a wideband CP antenna | 154 |
| 6.15 | LHCP/RHCP reconfigurability implemented into the E-shaped patch design . . | 155 |
| 6.16 | Reconfigurable E-shaped patch implementation for polarization reconfigurability using MEMS switches | 156 |
| 6.17 | Possible designs which violate a constraint. It is desired to avoid these designs due to possible fabrication issues or to avoid distortions to the E-shaped design . | 159 |
| 6.18 | Convergence of the CP E-shaped patch design optimization | 164 |

| | | |
|------|--|-----|
| 6.19 | Comparison of the impedance matching performance for the CP E-shaped patch antenna between the circuit simulation model, full MEMS simulation model, and a measurement of a fabricated CP E-shaped patch antenna with wirebonded MEMS shown in Figure 6.20 | 165 |
| 6.20 | Fabricated CP E-shaped patch antenna with wirebonded MEMS switches for port and radiation pattern measurements | 165 |
| 6.21 | Comparison of the axial ratio for the CP E-shaped patch antenna between the circuit simulation model, full MEMS simulation model, and a wirebonded MEMS measurement shown in Figure 6.20b | 167 |
| 6.22 | Principal patterns for the fabricated RHCP/LHCP reconfigurable E-shaped patch antenna with wirebonded MEMS switches at 2.45 GHz. Its directivity is $D_0 = 8.34$ dB. | 167 |
| 6.23 | Depiction of the slot modes and the effect of changing slot dimensions on the resonant frequency | 170 |
| 6.24 | Reconfigurable E-shaped patch implementation for frequency reconfigurability using MEMS switches | 172 |
| 6.25 | Convergence of the frequency reconfigurable E-shaped patch design optimization | 178 |
| 6.26 | Comparison of the impedance matching performance for the frequency reconfigurable E-shaped patch antenna between the circuit simulation model, full MEMS simulation model, and a fabricated E-shaped patch antenna with wirebonded MEMS shown in Figure 6.27 | 180 |
| 6.27 | Fabricated frequency reconfigurable E-shaped patch antenna with wirebonded MEMS switches | 180 |
| 6.28 | Simulated (circuit model) and measured frequency reconfigurable E-shaped patch antenna patterns at 2.55 GHz in the principle planes. The directivity $D_0 = 10.57$ dB for this frequency. | 181 |

| | | |
|------|---|-----|
| 6.29 | Comparison of the impedance matching performance for the simulation with no bias lines, the simulation with metallic lines included, and the measurement with metallic lines included as depicted in Figure 6.30 | 183 |
| 6.30 | Simulated and fabricated models to test metallic bias networks | 183 |
| 6.31 | Comparison of the effect of line length, shown in Figure 6.32, on S_{11} performance in order to determine whether a resonant line causes the impedance mismatch . | 185 |
| 6.32 | Simulation model used to determine the dependence of S_{11} on the length, d , of the bias line | 185 |
| 6.33 | Simulation models to compare a bias line with gaps (open circuit) and 10 k Ω resistors filling the gaps | 187 |
| 6.34 | Comparison of the S_{11} performance for the simulation with no bias lines, the simulation with metallic lines with gaps shown in Figure 6.33a, and the simulation with resistors shown in 6.33b | 187 |
| 6.35 | Fabricated E-shaped patch antenna with metallic bias lines connected by 8 SMT 10 k Ω resistors, where the total line resistance should be roughly 80 k Ω | 189 |
| 6.36 | Comparison of the impedance matching performance simulation and measurement results for 2 cases: the E-shaped patch design with metallic bias lines having gaps and the same design with 10 k Ω resistors filling gaps | 189 |
| 6.37 | Comparison of the impedance matching performance for the simulation with no bias lines (Figure 6.38a), the measurement without bias lines (Figure 6.38b), and the measurement with lossy lines included (Figure 6.38c) | 191 |
| 6.38 | Simulated and fabricated models to test lossy bias line networks | 191 |

LIST OF TABLES

| | | |
|-----|---|----|
| 2.1 | Recommended Values for the Intrinsic Parameters of PSO when used in Electromagnetics problems | 33 |
| 2.2 | Recommended values for the CMAES technique | 47 |
| 2.3 | Intrinsic Parameters Used to Optimize the 2D Schwefel Function | 53 |
| 3.1 | Benchmark Testing Functions | 60 |
| 3.2 | PSO Intrinsic Parameters for $N = 50$ | 61 |
| 3.3 | CMAES Intrinsic Parameters for $N = 50$ | 61 |
| 3.4 | PSO Intrinsic Parameters for $N = 5$ | 67 |
| 3.5 | CMAES Intrinsic Parameters for $N = 5$ | 67 |
| 3.6 | PSO Intrinsic Parameters for the Nonuniform Array Optimization | 73 |
| 3.7 | CMAES Intrinsic Parameters for the Nonuniform Array Optimization | 74 |
| 3.8 | Final Design Values provided by CMAES and PSO in the Nonuniform array optimization | 76 |
| 4.1 | Average Values for Design Objectives | 87 |
| 4.2 | PSO Intrinsic Parameters for XPFO | 89 |
| 4.3 | CMAES Intrinsic Parameters for XPFO | 89 |
| 4.4 | Final Design Values provided by CMAES and PSO in the XPFO | 91 |
| 4.5 | Pattern Characteristics of the XPFO Final Design | 92 |
| 4.6 | Average Values for Design Objectives in the BWFO runs | 95 |
| 4.7 | PSO Intrinsic Parameters for BWFO | 98 |
| 4.8 | CMAES Intrinsic Parameters for BWFO | 98 |
| 4.9 | Final Design Values provided by CMAES and PSO in the BWFO | 99 |

| | | |
|------|---|-----|
| 4.10 | Pattern Characteristics of the BWFO Final Designs | 101 |
| 4.11 | Final Design Values provided by PSO in the Optimization Runs | 103 |
| 4.12 | Pattern Characteristics of the BWFO Final Designs | 103 |
| 5.1 | Design Specifications for both the Stepped and Sigmoid Septum designs in terms of free space wavelength λ_0 at 5.8 GHz | 119 |
| 5.2 | PSO Intrinsic Parameters for the Stepped Septum Optimization using Six Steps | 126 |
| 5.3 | Final Design Values from the Stepped Septum Optimization | 127 |
| 5.4 | Final Design Values from the Stepped Septum Optimization | 132 |
| 5.5 | PSO Intrinsic Parameters for the Sigmoid Septum Optimization using 6 Sigmoids | 133 |
| 6.1 | Average Values for Design Objectives | 161 |
| 6.2 | PSO Intrinsic Parameters for the RHCP/LHCP Reconfigurable E-shaped patch antenna design optimization | 162 |
| 6.3 | Final Design Values from the CP E-shaped Patch Optimization | 164 |
| 6.4 | PSO Intrinsic Parameters for the Frequency Reconfigurable E-shaped patch an- tenna design optimization | 176 |
| 6.5 | Final Design Values from the FR E-shaped Patch Optimization | 178 |

ACKNOWLEDGMENTS

I would like to acknowledge and thank Shubhendu Bhardwaj, Ilkyu Kim, and Harish Rajagopalan from the UCLA Antenna Research, Analysis, and Measurement Laboratory for their help in preparing this thesis as well as their collaboration on the various projects conducted during my Masters at UCLA. A special thanks also to Timothy Brockett for his help with many of the measurements presented in this thesis.

I am sincerely grateful to Prof. Tatsuo Itoh and Prof. Lieven Vandenberghe for their time and energy spent as part of my thesis committee. I am also forever indebted to Prof. Yahya Rahmat-Samii's support, guidance, wisdom, and time given towards furthering my education and teaching me how to become a better researcher.

CHAPTER 1

Introduction

The continuous technological advancement of wireless communication and radar systems has increased the complexity of design constraints as well as performance evaluation for antenna designs. For practicing engineers there are often two options to deliver a final antenna design when the classical textbook designs are not sufficient. The first is to develop an antenna using a canonical shape thereby allowing exact mathematical analysis. This can be quite painstaking and rigorous, and it is often impossible to solve for non-canonical geometries, therefore limiting its applicability. The second option is to use *trial-and-error* techniques, which can be cumbersome and time-consuming. This approach can often lead to a characterization of the relationship between the design objectives and its design parameters, which is useful to engineers and can even aid in developing a theoretical analysis of the antenna structure. Yet, without any *a priori* knowledge on the antenna structure and its physical mechanisms, one may need to conduct an extraordinarily large number of simulations, which can be time consuming. In many cases, there can exist objectives which may have no easily seen correlation to the design objectives as will be seen in Chapter 4.

Therefore, in order to address the challenges and requirements presented by these sophisticated electromagnetic systems, there is a need to develop novel antenna design solutions and strategies. One of the recently emerging approaches that has been proposed to tackle this problem in a systematic fashion is the amalgamation of nature-inspired optimization techniques with simulation models which output the performance evaluation for each particular test design. By combining electromagnetic simulation tools with global optimization techniques, one can reach an antenna design solution in an autonomous manner. These methods also do not require any *a priori* knowledge about the design. Certainly, nature-inspired optimization has been one of the

forefronts within electromagnetics research due to its widely proven abilities to solve complex problems that do not lend themselves to simple solutions.

This chapter is devoted to providing a brief motivational overview on the role of antennas in communication systems and radar. This serves to familiarize the reader with the significance of antennas in the overall system, thereby emphasizing the importance in conducting optimization. The next section then discusses the role of optimization within electromagnetics and provides some optimization examples. We conclude this chapter by defining many of the performance parameters that are important in optimizations for those that may be less familiar with electromagnetics and antenna engineering.

1.1 Motivation

Electromagnetics has given rise to the development of engineering systems over a wide range of applications. Communication and radar systems are among the leading technologies that have made a significant impact on society. With worldwide communication now readily available, one's local community in the surrounding area has now expanded to a global community, thus enabling more interaction across cultures. With this new enhancement a multi-cultural society begins to thrive as people learn more about other cultures that were previously inaccessible. Commerce is expanded to a global level that is more available to people of all socioeconomic status. The Internet, an innovative means of communication, has brought about revolutionary concepts such that it is now commonplace to have conversations with others halfway across the globe in real time for a low cost. The influence of these relatively newer means of communication have been far-reaching.

Wireless communication systems have been gaining more popularity due to their added versatility and flexibility. Recent advances in signal processing, microelectronics fabrication, and microwave system design have permitted the development of wireless systems operating at low power levels with minimal interference towards other devices under the same infrastructure. Among these are the cellular phone, WiMAX, WiFi, and 4G LTE systems. Indeed, newly proposed systems such as LTE-advanced aim to support systems with nearly 1 Gb/s downlink and

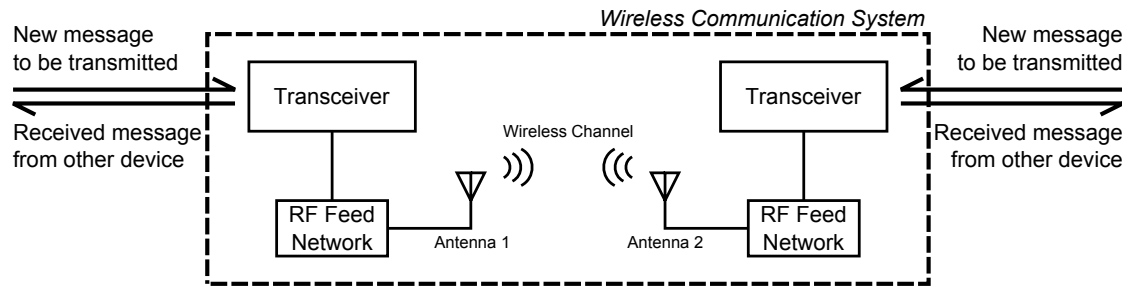


Figure 1.1: Depiction of the basic blocks of a wireless communication system

500 Mb/s uplink [1]. These systems could not have been developed without the use of signal processing, communication theory, and ultimately electromagnetics.

Wireless systems are also implemented for other non-multimedia applications that have aided in saving lives. Some systems provide a means of communication in disaster areas requiring immediate attention and help responders pinpoint the location with the most need. The development of systems that can operate under harsh conditions or even in remote areas is a challenging task [2], and several organizations such as UNICEF have created projects to develop new systems that can increase communications in isolated areas [3]. Others have approached the problem by developing low altitude balloon-based WiFi systems that are capable of covering a 5.5 km radius [4]. These are only some of the many interesting examples of applications using wireless communication systems. There still remains a much greater variety of applications that would take a whole volume of books to cover every possible wireless communication system that has been developed.

As engineers, we are interested in the technical aspects of the communication system. A high level block diagram of a duplex wireless communication system is shown in Figure 1.1. It is often the role of computer engineers, communication engineers, and embedded system designers to create a user interface to the transceiver. With this interface, one can then either transmit or receive messages via the wireless communication system. The transceivers within this system block perform several functions which often include message encoding/decoding, channel encoding/decoding, error coding, and modulation/demodulation for a digital system [5]. While the previously mentioned components are key to the success of a communication system, the propagating electromagnetic wave still serves to carry the message from the transmitter to the

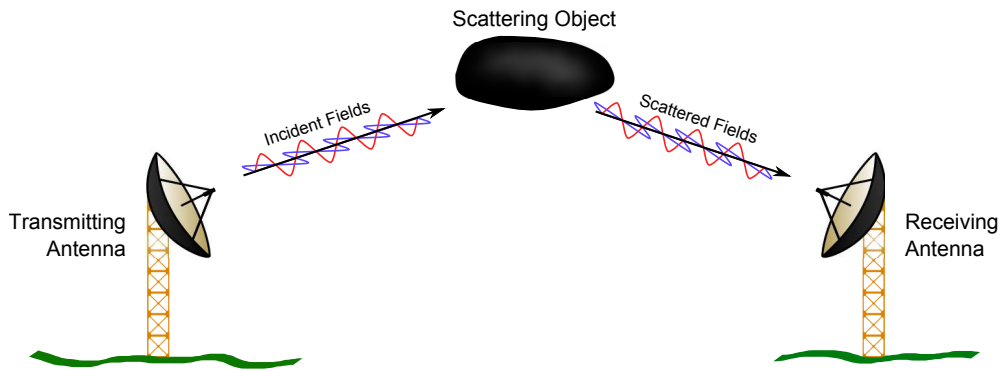


Figure 1.2: Basic bistatic radar system detecting a scattering object

receiver. Therefore it is extremely important to design properly a system which manipulates the electromagnetic fields in a way such that the SNR is maximized, thus emphasizing the significance of a proper antenna design.

A radar system's primary goal is to identify or characterize objects or materials in a given area of interest. It accomplishes this in various ways, but the most widely recognized form is through the measurement of the backscattered fields, or radar cross section (RCS). In the most basic sense, a radar system transmits electromagnetic waves which impinge upon an object if present. This object scatters the incident waves, and these scattered fields can be received by a receiving antenna (bistatic radar) or by the original transmitting antenna (monostatic). This basic system is depicted in Figure 1.2, where the transmitting antenna radiates an electromagnetic wave and the receiving antenna measures the backscattered fields. If no object is present (or if the RCS is small), then the measured fields will be minimal. For military applications, the aim is to identify possible incoming threats or targets. For scientific and space applications, radars can provide new scientific data, giving scientists valuable information about world climate, fresh water supply, sea level, sea-ice mapping, precipitation, and storms.

Several space missions sponsored by the National Aeronautics and Space Administration (NASA) provide interesting examples of radar applications. One example is CloudSat, a NASA mission deployed to investigate cloud behavior and its effect on climate. It is equipped with a 94 GHz nadir-looking radar that observes the backscattered radiation from the clouds. With these measurements scientists believe that they will be able to advance our knowledge on cloud abundance, structure, and radiative properties. Ultimately this will enable researchers to better

understand the exchange of solar and thermal energy between the atmosphere, hydrosphere, land surface, biosphere, and space [6]. Another mission that was joint between NASA in the United States and the Deutsche Forschungsanstalt für Luft und Raumfahrt (DLR) in Germany was the Gravity Recovery and Climate Experiment (GRACE) mission. This mission aimed to finely map the Earth's gravitational fields using both a GPS and microwave ranging system. This data can then be used to study changes in the Earth's gravity field due to surface and deep currents in the ocean, variations of mass within the Earth, exchanges between glaciers and the ocean, and ground water storage on land masses [7, 8]. Some other future and current NASA missions using radar technologies also include Aquarius [9], Soil Moisture Active Passive (SMAP) [10], and the Gravity Recovery and Interior Laboratory (GRAIL) mission [11].

From these brief discussions, one can recognize the significance of antennas to wireless communication and radar system performance. It is common for these systems to operate with strict design specifications on parameters such as high bandwidth and low cross-polarization radiation. This can make it difficult to meet with standard antenna designs, and therefore new designs are a must. It is common for the RF feed networks and the antennas to operate at relatively high frequencies in the 100 MHz to 100 GHz range. Operation at these frequencies necessitates the use of advanced electromagnetic theory in order to properly characterize the microwave feed network. The radiative properties of the antenna also require the use of these advanced theories for analysis. This theoretical framework does not always lead to a solution that is easily identifiable, and therefore optimization can be applied to provide a final design solution which provides optimal performance for the system.

Modern electromagnetic theory is embodied by Maxwell's equations, which are the characteristic equations that define electromagnetic waves and radiation and are shown in the following

equations. These equations have been discussed in [12] as well as many other textbooks.

$$\nabla \times \vec{E} = -\frac{\partial \vec{B}}{\partial t} \quad (1.1a)$$

$$\nabla \times \vec{H} = \vec{J} + \frac{\partial \vec{D}}{\partial t} \quad (1.1b)$$

$$\nabla \cdot \vec{D} = \rho \quad (1.1c)$$

$$\nabla \cdot \vec{B} = 0 \quad (1.1d)$$

In Equation 1.1, \vec{E} represents the electric field, \vec{B} is the magnetic flux density, \vec{H} is the magnetic field, \vec{J} is the electric volume current density, \vec{D} is the electric flux density, and ρ is the electric charge density. Assuming linear, isotropic, and homogenous media, we also have the constituent equations given as

$$\vec{B} = \mu \vec{H} \quad (1.2a)$$

$$\vec{D} = \varepsilon \vec{E} \quad (1.2b)$$

where μ is the permeability of the medium and ε is the permittivity of the medium. With equations 1.1 and 1.2 we have vector partial differential equations in which the variables of interest, \vec{E} and \vec{H} , are also coupled. From these equations we can observe the analytical challenges inherent in the analysis of radiating antenna structures. With such complex equations, scientists are often limited to solve only canonical geometries using exact analysis such as dipole or loop antennas [13, 14, 15]. At times approximations can be made if the antenna structure only slightly deviates from these geometries. For the most general structures, researchers forego exact analysis and utilize numerical algorithms in order to characterize the antenna performance. While numerical analysis can significantly aid in evaluating the performance of a structure, it cannot provide exact analysis which relates the geometrical parameters to the antenna performance. Therefore researchers often resort to *trial-and-error* techniques in order to find a good design (if one exists).

These *trial-and-error* techniques can provide a great deal of information to the investigator, but it can often be quite time-consuming in order to properly search the space with uniformly

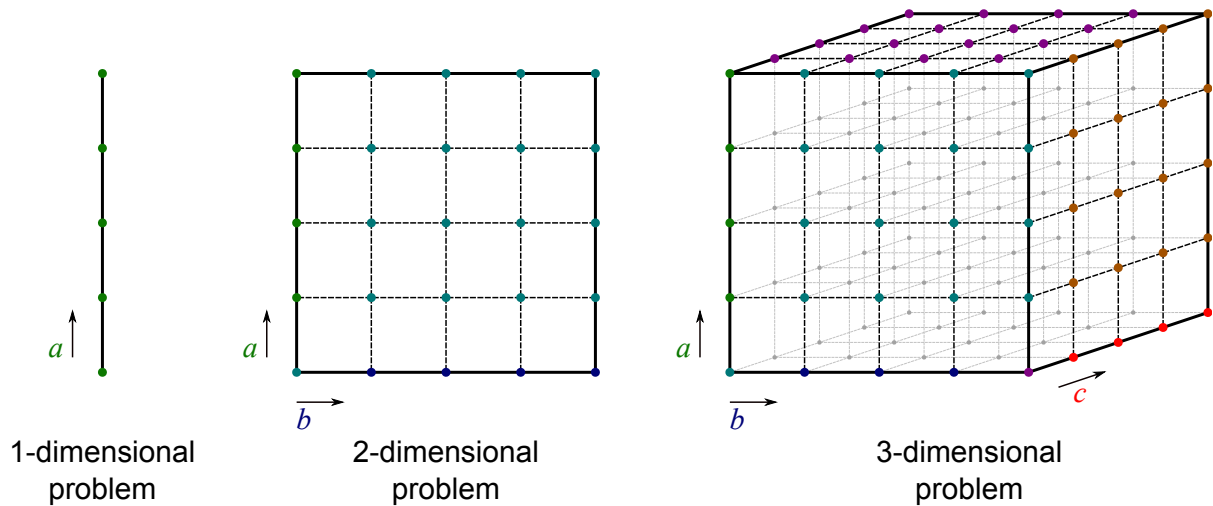


Figure 1.3: Representation of design parameters with uniformly spaced testing points for 1 dimension, 2 dimensions, and 3 dimensions

spaced testing points. This technique only works well for cases involving a small number of parameters, but a different approach is needed for highly dimensional problems involving tens or hundreds of variables. Figure 1.3 shows how an increase in the dimensionality increases the number of points to be tested. With highly dimensional problems, the number of test points increases exponentially, therefore making the overall time required very lengthy. For example, suppose an antenna design had 5 variables that needed to be given values, and *trial-and-error* was used to search the possible solution space. Assuming that 10 points per dimension was used, then a total of 10^5 solutions would be tested. A typical simulation time for numerical electromagnetic simulation tools is on the order of a few minutes, and therefore we assume a 3 minute simulation time for demonstration purposes. The total time needed for the *trial-and-error* testing would be 3×10^5 minutes, which translates to roughly 208 days! Note that this is only for a 5-dimensional problem, which is not necessarily a highly-dimensional problem. Imagine the length of time for a 25-dimensional or even 100-dimensional problem. The length of time needed to search the solution space uniformly could be well beyond one's lifetime, which can hinder further research.

In this context, optimization can offer a significant advantage for these types of design problems where no *a priori* knowledge is given. The primary difference between an optimization versus *trial-and-error* techniques is that the optimization guides the new points to be tested

based on previous performance evaluation. This knowledge can significantly reduce the amount of time to get to a good solution, and there exist many different types of optimization techniques discussed in Section 1.2 which use this information in different ways. Many times a design has a specific requirement that indirectly relates to the more common antenna performance parameters. These parameters may be non-intuitive and might not provide a clear relationship between the design parameters and the non-intuitive objective. In many cases designs have multiple criterion to meet, and this can make it difficult for designers to decide between certain solutions. This case is often referred to as a multi-objective optimization problem and are quite challenging to find a final design. For these reasons, one might choose optimization over *trial-and-error* and exact analysis.

1.2 Optimization in Electromagnetics

It should be emphasized that optimization is not a numerical solver for electromagnetics problems. It cannot be applied to solve Maxwell's equations for an arbitrary problem. Rather, it can be used in conjunction with other solvers that employ numerical techniques to solve Maxwell's equations such as the Method of Moments (MoM) [16, 17, 18], the Finite Element Method (FEM) [19, 20, 21], or the Finite-Difference-Time Domain (FDTD) method [22, 23, 24]. Each of these algorithms have their shortcomings as well as advantages over the others, but a discussion on the topics in numerical electromagnetics is out of the scope of this thesis. Instead, we approach design problems with the black box assumption; these algorithms have already been well established for computing antenna parameters of interest in the optimization and no further details are necessary for the construction of the optimization run. There may be some occasional discussions on the choice of numerical algorithm due to speed considerations, but this will usually be the farthest extent of our discussion on these algorithms.

Some researchers have presented numerical techniques involving nature-inspired optimization having the appearance of a numerical solver for Maxwell's equations, but this impression is not the most accurate one. These new techniques involving nature-inspired optimizers provide simplified models of antennas using infinitesimal dipole models [25]. They can provide a fast

analytical alternative in comparison to the techniques previously mentioned, and many parameters which may have been difficult to simulate are now achievable at low computational cost. This technique has been applied to design problems for aperiodic arrays [26] as well as MIMO systems [27]. The approach is to place infinitesimal dipoles in the same volume containing the antenna. The near fields along an observation plane are assumed to have been computed by a MoM simulator for the original antenna of interest. An optimizer is then used to find the coefficients of the dipoles and their locations in space by comparing the near field data given by MoM and the dipole near fields. While this might suggest that it is another approach to solving far-fields/near-fields of an antenna, the approach's use of optimization is more reminiscent of solving inverse problems $\mathcal{L}[f] = g$, where the source vector f is found by optimization techniques. If the dipoles' location is also being optimized then both the operator \mathcal{L} and the source vector f are being optimized to finally equate to the simulated observation vector g , and this operation conducted by the optimization algorithm has the same function as a matrix inversion, which is still a difficult problem to solve. This hereby reinforces our original statement that these optimization techniques do not solve Maxwell's equations but rather can be used as tools in the process.

By necessity we incorporate these techniques (MoM, FEM, FDTD) into the optimization algorithm in order to link Maxwell's equations to the optimizer. Figure 1.4 demonstrates the typical work flow for an electromagnetic optimizer. The steps below give a foundation for developing an optimization run for a given design [28]. Steps 1-3 are encompassed by the *Establish parameters* box, and steps 4-5 are embodied by the three box cycle which continues until the design meets the objectives. Note that the bird, people population, and DNA strands are often logos representing the Particle Swarm Optimization (PSO), Evolutionary Strategies (ES), and Genetic Algorithms (GA) techniques, which are popular nature-inspired techniques for electromagnetics applications.

1. **Defining the optimization problem.** The first step in the optimization is to define the problem, which can involve defining the antenna topology as well as the parameters of interest. These parameters can vary from application to application, and Section 1.3 will discuss more on the various aspects of antennas that are of interest. At this step, many assumptions can be made which can greatly enhance the convergence of the optimization,

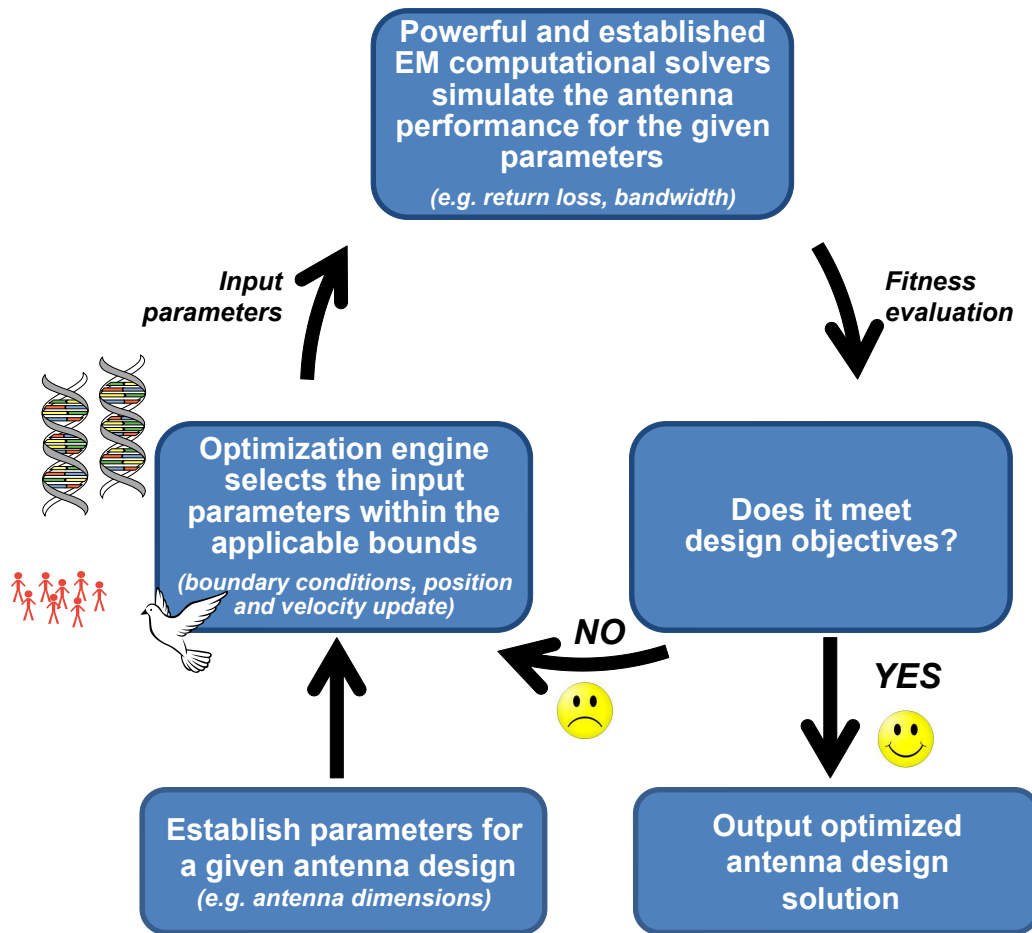


Figure 1.4: Typical flowchart for an optimization algorithm for electromagnetic design problems

and it is the antenna designer’s task to minimize the number of variables to optimize. For instance, one could use a completely generalized topology defined by pixels, but this represents a highly multidimensional binary optimization problem which is extremely difficult to optimize. These types of runs are only encouraged when high performance demands are required and no topology demonstrates adequacy. Sometimes these optimizations are used because of their generality, and it can demonstrate limits for possible applications.

2. **Defining the algorithm parameters.** Many optimization techniques have intrinsic parameters that must be specified in order to proceed. Some of these can be solution space boundaries, mutation operators, particle velocities, and many others. Researchers in the evolutionary computation field have been working to develop codes where the intrinsic parameters are predefined (or are adaptive) and do not require any user input. Other techniques still require these parameters, and thus this step still remains an important one in an optimization.

3. **Define a *fitness function*.** In order to optimize a design, one must characterize the parameter(s) of interest that are important in the design specifications. In the optimization community, this is known as either a cost function or fitness function, and it represents a performance measurement. For multi-objective optimizations, this can be represented by a vector function, and for single-objective optimizations this is represented by a scalar function. In general, multi-objective optimizations can take longer than their single-objective counterparts, and therefore one can use a linear transformation, $f = \vec{w}_g^T \vec{g}$, to make a multi-objective optimization a single-objective one. In this equation, f represents the fitness function, \vec{w}_g^T is the weighting vector which properly weights the optimization goals, and \vec{g} is a vector representing the goals (parameters) of interest in the optimization.
4. **Initialize test points.** There are different techniques on how to initialize the test solutions, and most nature-inspired optimization techniques randomly generate starting points based on a given solution space. Some use uniformly distributed initialization points whereas others might use gaussian distributed initialization points. Derivative-based methods typically require some *a priori* knowledge which places the test points near the global optima, otherwise the algorithm might converge upon local optima.
5. **Systematically search the solution space.** This step and its substeps distinguish each algorithm from the others. This section defines how each algorithm uses the previous points to choose for the next iteration. Nature-inspired optimizers typically generate the next set of test points by a randomly generated shift in space with the distribution controlled by previous observations. Gradient based methods typically are directed towards zero-derivative points from quadratic approximations given by a Hessian matrix.
 - (a) *Evaluate the fitness function.* The fitness function for each testing point is computed by numerical techniques (MoM, FEM, FDTD) and then output as a single number (single-objective) or as a vector (multi-objective). This is often the most time-consuming component depending on the antenna geometry of interest. If there are additional engineering constraints, then these are sometimes incorporated into the fitness function by adding penalty functions [29].
 - (b) *Test convergence criterion.* There are many stop criterion for optimization. A simple one that is often used is a maximum number of iterations. One can either stop the optimization if the performance parameters satisfy the criterion desired or if the optimization shows no significant progress over the past few iterations. For the latter, a certain tolerance δ is often provided, and the optimizer stops when the fitness does not change by more than δ over a certain number of iterations.
 - (c) *Select the next values to be tested.* Choosing the next solutions to be tested is always dictated by the optimization algorithm. For this particular thesis, we will go over two nature-inspired optimization algorithms, and Chapter 2 will discuss the details on how these two algorithms choose the next points.

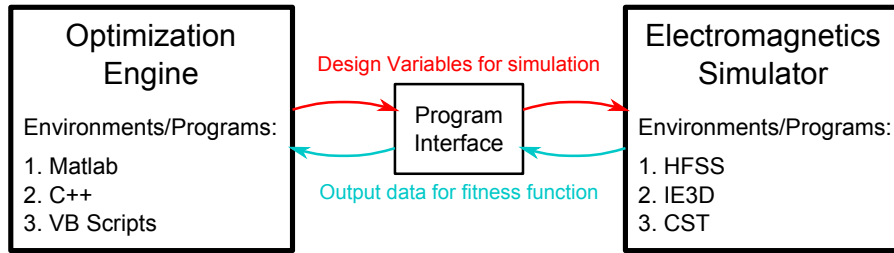


Figure 1.5: Interface configuration for the simulator and the optimization engine

The flowchart in Figure 1.4 and the generalized steps shown above provide only a high level understanding to the optimization process as a whole. With this big picture in mind, we can proceed to discuss the details of each step in the proceeding chapters. We also see from this generalized framework that it is rather straightforward to apply optimization to antenna designs. Once we have a numerical model that accurately outputs the desired antenna parameters, we can establish a program interface which connects the numerical solver to the optimizer as shown in Figure 1.5. The red connections depicted represent the optimizer providing the design variable values to the simulation tool, and the cyan colored arrows represent the output data being given to the optimizer for the computation of the fitness. Once this connection is made then one can proceed forward with the optimization.

There are infinitely many applications where optimization could improve designs for electromagnetic systems, and it also has a rich history leading up to the use of nature-inspired optimization techniques. Optimization has played a major role in electromagnetics, and in the early days the standard gradient based techniques such as the generalized Newton-Rhapson or the Steepest Descent techniques were primarily used [30]. Other techniques which did not require derivatives include the nonlinear simplex method and the pattern search technique [30]. Several examples of common optimization problems in electromagnetics during the 1960-1970s include microwave circuit design [31] and antenna array design [32]. Of course these are only a few representative examples of applications using classical optimization techniques, and by no means is this list exhaustive. In Chapter 2 there will be a further discussion on the categorization of the different optimization techniques. One of the first published uses of nature-inspired algorithms in electromagnetics began with the use of Simulated Annealing (SA) in 1983 for image reconstruction in coded-aperture imaging and its following applications to optical image

reconstruction [33, 34, 35]. Later these techniques were applied to microwave imaging in 1991 [36]. Nature-inspired optimization techniques started being applied to antenna design problems when SA was used in the design of correlation antenna arrays [37] in 1988. Around the same time, Evolutionary Strategies (ES) was being applied in 1989-90 to the design of magnets used in Nuclear Magnetic Resonance applications [38, 39, 40]. Research in nature-inspired optimization for antenna applications lay dormant for a few years until Genetic Algorithms (GA) was introduced to the electromagnetics community in its application to broadband, lightweight microwave absorber [41] in 1993. After this awakening, a few significant papers were written on the application of GA to general electromagnetics problems [42, 43, 44].

This began the era where nature-inspired optimization techniques were gradually accepted into the electromagnetics community as a viable option to provide final antenna design solutions, and many other techniques have been introduced other than SA and GA since then. At this present time, it would be impractical to list all applications that have been researched in the literature. Therefore, the following bullets provide several major areas to which researchers have applied nature-inspired optimization algorithms.

- Antenna array nulling [45, 46]
- Thinned arrays [47, 48]
- Ultra-Wideband (UWB) antennas [49, 50]
- Reflector Shaping [51, 52]
- Yagi-Uda antennas [53, 54]
- Radar absorbing material (RAM), microwave absorbers [41, 48, 55]
- Pixelated patch antennas [56, 48]
- Frequency selective surfaces (FSS) [57, 58]
- Antennas for wireless communications [59, 60]

This list provides a brief glimpse into many of the applications which optimization has aided researchers in electromagnetics, and there exist many other projects which would take many

book volumes to list. Yet, there still remain many new exciting discoveries yet to be made through the application of optimization towards electromagnetic problems.

1.3 Performance Evaluation in Antenna Design

It is important to remember that the most time consuming component in the optimization algorithms (and even in the *trial-and-error* technique) is the *fitness function* evaluation. The fitness function defines the link between the physical system and the optimizer, and it describes the performance of a given design with a single number (single objective) or a vector (multi-objective). This function represents the performance for a given set of parameter values, and one must develop a fitness function that allows the optimizer to distinguish better designs from unsuitable ones [28]. Therefore, it is imperative to understand the antenna performance characteristics. Otherwise an erroneous understanding can lead to designs that do not meet the specifications desired. It is also the case that a good understanding of the antenna properties can lead one to develop performance evaluation functions which can be less time-consuming. This can be done by a clever formulation or by an assumption which holds for a particular design.

In wireless communication systems, the antenna link and electromagnetic wave propagation represents the system channel, as shown in Figure 1.1. Therefore, the primary goal is to maximize this link despite the poor quality of typical wireless channels. Typically the parameters of interest to the system designers include the operational frequency, bandwidth, and the expected received signal-to-noise (SNR) ratio at the receiver. From the system perspective, the operational carrier frequency is typically determined by the spectrum allocated to that system and often is a predetermined value. The system bandwidth directly affects the available data rate, and the maximum bandwidth in the available frequency band is typically desired. The received SNR directly determines the bit error rate (BER), which in most cases decreases as the SNR increases [5, 61]. By decreasing the BER, one can achieve less communication errors and better overall system performance, which is the general goal of the systems engineer.

For many antenna designs, there is a bi-directional relationship between the parameters and the antenna design. For instance, the operational frequency typically determines the smallest

antenna dimensions possible from the classical antenna design perspective. For a given frequency f , the antenna design dimensions are often near $\lambda/2$, where $\lambda = c/f$ is the wavelength in the antenna medium and c is the speed of light. In the reverse sense, one can find the operational frequency of an antenna design for a given resonant dimension $\ell \approx \lambda/2$. To this end, a knowledge of one parameter will typically dictate the other's value.

The SNR is often the most important parameter that guides the antenna designer, and electromagnetic theory must be utilized to characterize the communication link that results from a given design. For line-of-sight (LOS) applications where the electromagnetic radiation from the transmitter has a clear unobstructed path to the receiver, this can be done using the Friis transmission equation as shown below [15].

$$\frac{P_r}{P_{in}} = \left(\frac{\lambda}{4\pi r} \right)^2 G_{abs,t}(\phi_t, \theta_t) G_{abs,r}(\phi_r, \theta_r) |\hat{\rho}_t \cdot \hat{\rho}_r|^2 \quad (1.3)$$

In this equation we can find the ratio of the power received by the load, P_r , to the power input to the antenna, P_{in} . This ratio is defined by the Friis equation above and can be computed with the knowledge of the free space wavelength λ , the distance r between the antennas, the receiving antenna's absolute gain $G_{abs,r}$, the transmitting antenna's absolute gain $G_{abs,t}$ [15], and the polarization loss factor (PLF) $|\hat{\rho}_t \cdot \hat{\rho}_r|^2$. This is depicted by the antennas in Figure 1.6.

It should be noted that this equation is only valid for free space, but it can be used as an rough approximation to the antenna connectivity in the case where ground (often represented by a lossy dielectric [62]) and other objects are included in the scenario. Objects such as the ground can often be modeled as simple scattering structures, and a geometrical optics and geometrical theory of diffraction approach can be used to compute the interference and total signal level at a particular point. Despite the improvement in accuracy that this technique provides, it is extremely environment dependent, and even slight changes can alter the results. One could always optimize for the most typical scenarios encountered, but from the optimization viewpoint this technique is far too profuse for consideration. Rather, one could approach this problem by optimizing the system parameters that can improve the signal level for the average scenario. One begins from this perspective by asking what parameters in equation 1.3 could improve the

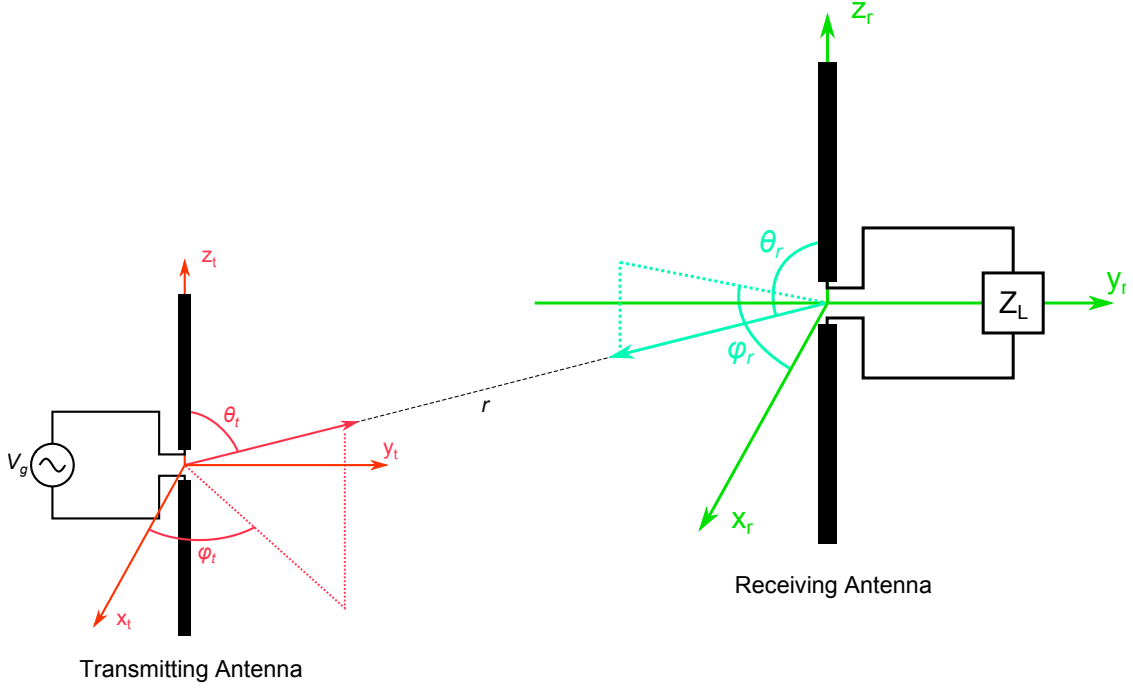


Figure 1.6: Transmitting and receiving antennas in free space

signal accordingly for a given arrangement of objects as well as antenna position and orientation. The parameters λ and P_{in} are often dictated by the system regulations and assigned frequency band, and the PLF ($|\hat{\rho}_r \cdot \hat{\rho}_t|^2$) and the distance r are defined by the given antenna positions and orientation. The only parameters left for optimization are the absolute gains, $G_{abs,r}(\phi_r, \theta_r)$ and $G_{abs,t}(\phi_t, \theta_t)$, and it has been standard practice in the antenna engineering community to optimize the absolute gain for the best guaranteed performance on the average.

At this point we will only focus on one antenna at a time for optimization purposes. The absolute gain for an antenna can be broken down into several major components as shown in the equation below [15].

$$G_{abs}(\phi, \theta) = e_{cd} (1 - |\Gamma|^2) D(\phi, \theta) \quad (1.4)$$

Here e_{cd} represents the conductor-dielectric efficiency which represents the power lost to losses in the conductor or dielectric materials. The term Γ represents the impedance matching of the antenna given by

$$\Gamma = \frac{Z_{in} - Z_0}{Z_{in} + Z_0} \quad (1.5)$$

where Z_{in} is the antenna input impedance and Z_0 is the characteristic impedance of the transmission line providing electromagnetic power to the antenna [15]. This quantifies the magnitude of the reflected waves which appear in order to satisfy the impedance boundary condition at the load. These reflected waves represent losses in the power transmitted by the antenna with the term $(1 - |\Gamma|^2)$ [63]. The last term in equation 1.4 is $D(\phi, \theta)$, which is the antenna directivity in the (ϕ, θ) direction. The antenna directivity describes the amount of power is radiated in a particular direction in comparison to an isotropic antenna, which radiates equally in all directions. This provides a number which describes the nature of the radiation for that particular antenna for all angles in the spherical space ($\phi \in [0, 2\pi], \theta \in [0, \pi]$). The quantities D_0 and $G_{0,abs}$ commonly refer to the maximum directivity and absolute gain, respectively, and this notation will be used throughout this thesis. The maximums provide useful information about the radiation pattern in one number. More specifically, it specifies whether the antenna radiates in a few particular directions or more uniformly over the entire spherical space. We will often refer to e_{cd} , Γ , and Z_{in} as the antenna port parameters (or specifications), and $G_{abs}(\phi, \theta)$ and $D(\phi, \theta)$ are referred to as radiation parameters. This may be confusing since the absolute gain incorporates both port and radiation parameters, but this is a common notation since G_{abs} is simply the directivity scaled by its overall efficiency.

Each of these components have a unique dependence on frequency, and it is important to understand this relationship to frequency in order to obtain a useful criterion for antenna bandwidth. Antenna bandwidth can be stated in terms of the various components listed above, and in general bandwidth can be specified by all sorts of antenna parameters. The quote below from C. A. Balanis describes this rather well.

The bandwidth of an antenna is defined as the range of frequencies within which the performance of the antenna, with respect to some characteristic, conforms to a specified standard. The bandwidth can be considered to be the range of frequencies, on either side of a center frequency (usually the resonance frequency for a dipole), where the antenna characteristics (such as input impedance, pattern, beamwidth, polarization, side lobe level, gain, beam direction, radiation efficiency) are within an acceptable value of those at the center frequency.

C. A. Balanis, *Antenna Theory: Analysis and Design* [15]

For many antenna designs, the impedance bandwidth typically defines the antenna's upper

and lower limits of operation and is often the most restrictive bandwidth among the other components. Impedance bandwidth refers to the bandwidth in which the reflection coefficient is $\Gamma < 0.316$. This reflection coefficient is often provided using a decibel scale, which is computed by the following.

$$\Gamma_{dB} = 20 \log_{10} |\Gamma| \quad (1.6)$$

In the dB scale, the impedance bandwidth is then guided by the $\Gamma_{dB} < -10$ dB rule of thumb. Using the formula $(1 - |\Gamma|^2)$, a reflection coefficient $\Gamma_{dB} = -10$ dB implies that roughly 90% of the power is accepted by the antenna. It should be noted that hereafter the subscript *dB* will be dropped and will be implied by the units provided for the rest of the thesis.

As stated in the quote from Balanis, the bandwidth can be restricted by other parameters as well including polarization, radiation efficiency, directivity, etc. However, for certain computational electromagnetics programs, such as the High Frequency Structure Simulator (HFSS) tool [64], it can be computationally expensive to calculate any far-field parameters such as axial ratio or directivity versus frequency. Therefore, one tries to avoid these as much as possible in the fitness function evaluation. Yet, there are times where these parameters are required to meet a specification, and one must incorporate them into the fitness function. Some examples include antennas with wide impedance bandwidths whose radiation patterns can change versus frequency. Since the directivity directly affects the final power received as seen in equation 1.3 and 1.4, one must account for the directivity in that particular direction versus frequency, therefore one would include this in their fitness function.

Of the three components seen in equation 1.4, the impedance matching is almost always incorporated into the fitness functions. For antennas in wireless communications, the radiation pattern is not as much a concern as the impedance bandwidth and antenna radiation efficiency. In radar applications, the radiation pattern can be just as important as the impedance matching. In a nutshell, it is extremely important that all information concerning the scattered fields is extracted properly, and this requires good radiation and port characteristics. The conductor-dielectric efficiency is often not of high concern, and this term is typically above 90% unless lossy materials are present. As we can see from the discussion above, our primary concern will

be the impedance matching and the radiation patterns of the design antenna, and these are the parameters on which we will focus in the optimization problems. The next chapters will provide several illustrative and illuminating examples of antenna design optimizations which utilize either port parameters, radiation parameters, or a mixture of both.

1.4 Outline of Work

In this thesis, two nature-inspired algorithms will be introduced and compared, and several optimization problems will be solved using these techniques. Figure 1.7 provides an illustration of the work flow in this document. First some brief background is given in this particular chapter (Chapter 1) with the goal to introduce the subject of optimization within the electromagnetics context and give a brief history on the many possible applications of antenna designs for communication systems and radar. Some of the parameters of interest to the antenna designer are also explained from the connectivity perspective using the well known Friis equation. These parameters will then be used in conjunction with numerical solvers in order to characterize the fitness a given design.

The next chapter will begin by defining the optimization framework to be used for the design problems. It provides definitions for the common terms to be used in connection with the global optimizers and describing the problem in general. The Particle Swarm Optimization and Covariance Matrix Adaptation algorithms will then be described, and some pseudocode is provided for a better picture on the implementation of the two algorithms. The last sections will discuss the additional features required for constrained optimization problems and also discuss the idea of convergence applied towards the nature-inspired algorithms.

Chapters 3 and 4 will compare the two algorithms for several different types of optimization problems. First, a comparison will be made using mathematical fitness functions which allow a quick simulation because the fitness function evaluation is computationally inexpensive. However, the optimization will be done in a resource limited setting, where the number of iterations/function evaluations is limited. An antenna array problem will also be provided in order to compare these two problems using an electromagnetics problem whose fitness can be evaluated

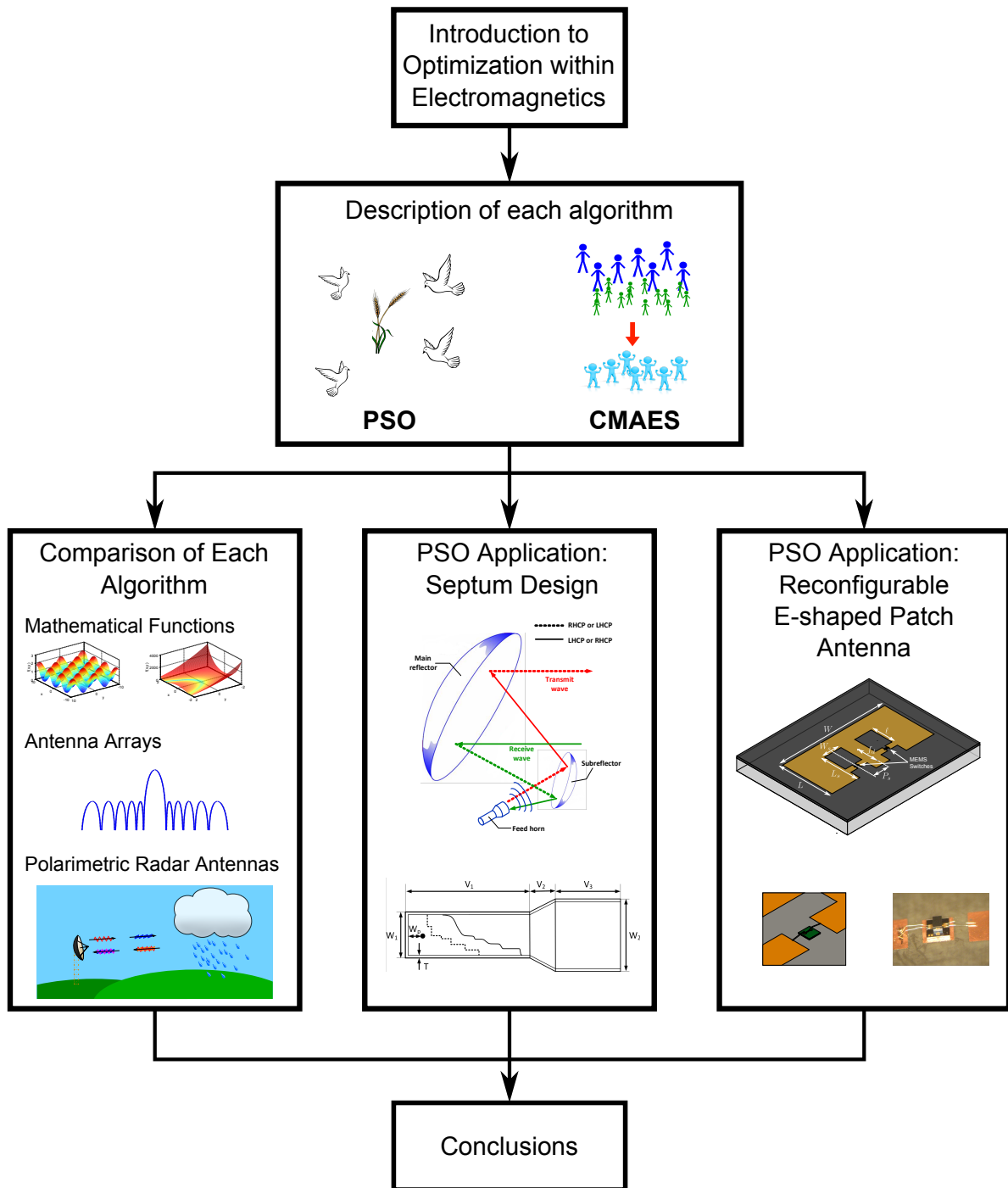


Figure 1.7: Outline of work in this thesis. The introduction to optimization within electromagnetics is given in Chapter 1. The comparison of the algorithms is given in Chapters 3 and 4. The septum design and the reconfigurable E-shaped patch designs are given in Chapters 5 and 6, respectively. The final conclusions are given Chapter 7.

quickly. The goal of this array problem is to minimize the sidelobe level in the sidelobe region by using a non-uniform array. In Chapter 4, the typical parameters in a dual polarize weather radar system are introduced and described, and the connection between the radar performance evaluation and the antenna parameters is given. Two different optimization formulas are used and each algorithm is used to optimize each type. In this chapter there are four optimization runs total, and comparison of the algorithms as well as the optimization formulation is provided.

Two septum designs are optimized using PSO in Chapter 5. The first is a standard stepped septum design commonly seen in the literature. A smoothed septum design using the Sigmoid function is also introduced for possible use in high power applications. These are both challenging highly dimensional optimization problems, and PSO is applied to provide good antenna performance over a specified frequency band in terms of the parameters discussed in Section 1.3. In Chapter 6, the E-shaped patch antenna concept is introduced and two possible reconfigurable E-shaped patch antennas are shown. A simple MEMS circuit model is given to simulate the performance of the reconfigurable antenna using MEMS switches. PSO is applied to both antenna designs to optimize the antenna performance. Bias network solutions are also provided to demonstrate the full implementation of the MEMS reconfigurable E-shaped patch antenna.